ENVIRONMENTAL RESEARCH
LETTERS

LETTER • OPEN ACCESS

Uncertainties in estimates of mortality attributable to ambient $PM_{2.5}$ in Europe

To cite this article: Jonilda Kushta *et al* 2018 *Environ. Res. Lett.* **13** 064029

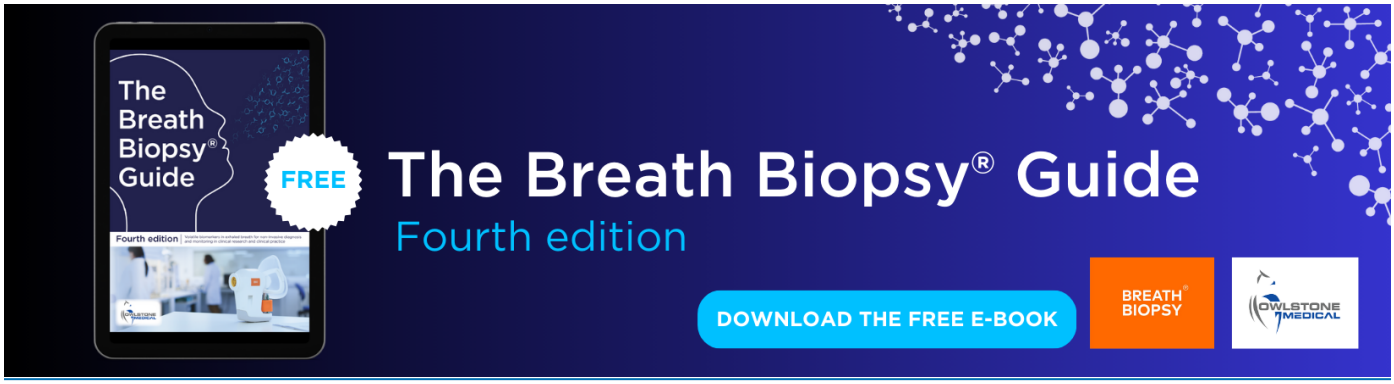

Environmental Research Letters

LETTER

Uncertainties in estimates of mortality attributable to ambient $PM_{2.5}$ in Europe

Jonilda Kushta[1,3], Andrea Pozzer[2] and Jos Lelieveld[1,2]

[1] Energy, Environment and Water Research Centre (EEWRC), The Cyprus Institute, Nicosia, 2121, Cyprus
[2] Max Planck Institute for Chemistry, Mainz, 55128, Germany
[3] Author to whom any correspondence should be addressed.

E-mail: j.kushta@cyi.ac.cy

OPEN ACCESS

RECEIVED
5 February 2018

REVISED
18 April 2018

ACCEPTED FOR PUBLICATION
18 April 2018

PUBLISHED
8 June 2018

Keywords: mortality estimates, regional atmospheric models, impact of aerosols on human health, uncertainties in $PM_{2.5}$

Abstract

The assessment of health impacts associated with airborne particulate matter smaller than 2.5 μm in diameter ($PM_{2.5}$) relies on aerosol concentrations derived either from monitoring networks, satellite observations, numerical models, or a combination thereof. When global chemistry-transport models are used for estimating $PM_{2.5}$, their relatively coarse resolution has been implied to lead to underestimation of health impacts in densely populated and industrialized areas. In this study the role of spatial resolution and of vertical layering of a regional air quality model, used to compute $PM_{2.5}$ impacts on public health and mortality, is investigated. We utilize grid spacings of 100 km and 20 km to calculate annual mean $PM_{2.5}$ concentrations over Europe, which are in turn applied to the estimation of premature mortality by cardiovascular and respiratory diseases. Using model results at a 100 km grid resolution yields about 535 000 annual premature deaths over the extended European domain (242 000 within the EU-28), while numbers approximately 2.4% higher are derived by using the 20 km resolution. Using the surface (i.e. lowest) layer of the model for $PM_{2.5}$ yields about 0.6% higher mortality rates compared with $PM_{2.5}$ averaged over the first 200 m above ground. Further, the calculation of relative risks (RR) from $PM_{2.5}$, using 0.1 $\mu g\,m^{-3}$ size resolution bins compared to the commonly used 1 $\mu g\,m^{-3}$, is associated with $\pm$0.8% uncertainty in estimated deaths. We conclude that model uncertainties contribute a small part of the overall uncertainty expressed by the 95% confidence intervals, which are of the order of $\pm$30%, mostly related to the RR calculations based on epidemiological data.

1. Introduction

Exposure to airborne fine particulate matter (diameter less than 2.5 μm, or $PM_{2.5}$) has been associated with a number of short- and long-term adverse health outcomes varying from respiratory illnesses to premature death (Dockery *et al* 1993, 2009, Pope *et al* 2002, 2004, 2009, Filleul *et al* 2005, Krewski *et al* 2009, Ostro *et al* 2010, Rückerl *et al* 2011, Beelen *et al* 2014). The assessment of health impacts from ambient (outdoor) air pollution relies on an integrated methodology that uses observations and/or air quality models to determine pollutant concentration distributions, and synthesizes this information with exposure and population vulnerability on national and global scales (Cohen *et al* 2005, Anenberg *et al* 2010, Li *et al* 2010, Pozzer *et al* 2012, Fann *et al* 2012, Lelieveld *et al* 2015, Giannadaki *et al* 2017, Pozzer *et al* 2017). The use of atmospheric modelling systems is necessary, in order to provide information on the $PM_{2.5}$ concentrations in regions where air quality is not monitored, and to investigate alternative scenarios related to factors such as emissions, air quality regulations and population development.

$PM_{2.5}$ concentrations are often derived from global models utilizing a grid spacing ranging from 100 km–400 km (Bey *et al* 2001, West *et al* 2006, Anenberg *et al* 2010, 2012). Many of the species that comprise a $PM_{2.5}$ total mass concentration are formed in the atmosphere from chemical reactions between precursor species (Thompson *et al* 2014). Strong spatial concentration gradients of emissions can influence chemical production, and may lead to errors at too coarse a resolution due to spatial

averaging of emissions (Thompson *et al* 2014). Thus, the use of coarse grid resolutions, necessitated by computational resource limitations and global model parameterisations, may result in the underestimation of peak concentrations in densely populated and industrialized areas (Punger and West 2013, Li *et al* 2010). This could influence mortality estimates by misrepresenting the gradients between pollution and population distributions, leading to errors in estimates of health impacts. Grid resolution is expected to affect differently the primary and secondary aerosols; therefore, an analysis of PM components instead of total particulates might be interesting (US EPA 2007, Punger and West 2013), warranting further investigation of spatial resolution to different airborne aerosol species. For applications on urban and regional scales, several studies have investigated how estimates of health impacts at coarser resolutions differ from those at fine resolutions (Punger and West 2013, Thompson *et al* 2014) with contradictory results. Punger and West (2013) reported that coarse grid resolutions produce national mortality estimates in the USA that are substantially low-biased. However, Thompson *et al* (2014) did not find a significant response of health impacts associated with changes in $PM_{2.5}$ concentrations to model resolution. A robust conclusion is pending.

In this study, we performed several sensitivity tests to identify the uncertainty range introduced to the mortality calculations related to the grid spacing of the modelling system, the vertical distribution of the $PM_{2.5}$ concentrations, and the bin size of the relative risk factor concentration step. We also calculated mortality rates from aerosol concentrations derived from satellite retrievals of the aerosol optical depth (AOD) for the same year (2014), from various satellite instruments (NASA MODIS, MISR, and SeaWIFS), as discussed in van Donkelaar *et al* (2016). Here we assess the relative differences between simulations and observational analysis relative to the 95% confidence interval in the estimation of the rates of mortality and disease, as derived from the epidemiological studies on the relative risk of disease.

This paper is organised as follows: section 2 gives a brief description of the methodology and tools used in this work. In section 3 the results of the uncertainties driven by the options used in the calculation of the mortality estimates are presented and discussed, while section 4 summarises the main findings of this work and proposes focus points for future analysis.

2. Methodology

We used the Weather Research and Forecast model coupled with Chemistry (WRF-Chem) version 3.6.1 to simulate particulate matter over Europe for the year 2014 (Grell *et al* 2005, Fast *et al* 2006). This modelling system includes meteorological and chemical modules that are fully consistent, as they apply the same transport scheme (mass and scalar preserving), physical schemes for subgrid-scale transport, and the same spatial and temporal configuration. WRF-Chem was configured over Europe and uses two domains, one with a horizontal resolution of 100 km and the other of 20 km, nested into the coarse grid domain. For both simulations, the following physical and chemical options are used. The second generation Regional Acid Deposition Model mechanism (Stockwell *et al* 1990) is applied to simulate the gas phase chemistry. The aerosol modules used are the Modal Aerosol Dynamics Model for Europe (Ackermann *et al* 1998) for inorganic species, and the Secondary Organic Aerosol Model (Schell *et al* 2001) for secondary organic aerosols. The aerosol size distribution is described with three log-normal modes (Aitken, accumulation, and coarse). The options for the physical parameterisations are the following: the Morrison microphysics scheme (Morrison *et al* 2005), the MM5 similarity surface layer scheme (Zhang and Anthes 1982), the Noah Land Surface Model (Chen and Dudhia 2001), the Yonsei University Planetary Boundary Layer scheme (Hong *et al* 2006), the Grell 3D Ensemble Scheme for cumulus parameterisation (Grell and Dévényi 2002), and the Rapid Radiative Transfer Model radiation scheme (Iacono *et al* 2008) for both shortwave and longwave radiation budgets.

The initial and boundary conditions for the meteorological data were provided by the National Center for Environmental Prediction global forecast system at a resolution of $0.5° \times 0.5°$. Land use and soil category data sets from the US Geological Survey (USGS) are used. The initial and boundary conditions for the chemical species are provided from global simulations with the Model for Ozone And Related chemical Tracers version 4 (MOZART-4) model (Emmons *et al* 2010). Emissions are calculated from the global emission dataset EDGAR-HTAP v2 (Janssens-Maenhout *et al* 2012). The EDGAR-HTAP dataset has a resolution of $0.1° \times 0.1°$ and provides annual anthropogenic emissions of NO_x, SO_x, non-methane volatile organic compounds (NMVOCs), CO, NH_3, $PM_{2.5}$ and PM_{10} covering 11 source sectors (SNAP categories), plus emissions from ships and volcanoes (SO_x) for the reference year 2010. In the EDGAR-HTAP v2 dataset, the NMVOCs are lumped into reactive compound categories, and the speciation into groups is based on the approach of Middleton *et al* (1990). Biogenic emissions (isoprene, monoterpenes and nitrogen emissions by soil) have been calculated on-line from the Model on Emissions of Gases and Aerosols from Nature, using the USGS land-use classification and branch-level emission factors which incorporate canopy shading.

The $PM_{2.5}$ concentrations derived from the two simulations are compared to measurements reported by European countries to the European Environment Agency (EEA) for 2014 and available in Airbase v. 8

(EEA 2016). The analysis covers all the regulated pollutants in the Air Quality Directives (EU 2004 and EU 2008) in the EU-28 and the European Economic Area member countries whose territories are fully included in the model domains. We use only those monitoring stations with at least 75% of data coverage (the fraction of the year for which valid concentration data is available) for the analysis of fine particles with diameters of 2.5 μm or less. Simulated mass concentrations of total $PM_{2.5}$ from anthropogenic sources (no mineral dust or sea salt) are then used to derive mortality estimates for several health conditions and age groups.

The diseases taken into account in this study include ischemic heart disease, cerebrovascular disease from ischaemic and haemorrhagic stroke, chronic obstructive pulmonary disease, lung cancer, and acute lower respiratory infections which also affect children. The methodology for the calculation of the mortality and incidence rates of the aforementioned diseases requires the input of spatially resolved $PM_{2.5}$ concentrations; these values are provided from the simulations of the WRF-Chem modelling system at 100 km and 20 km grid spacing covering the same region (Europe). The mass concentrations are given as annual means per grid cell (100×100 km and 20×20 km). No observational assimilation or calibration has been performed with ground-level $PM_{2.5}$ measurements or satellite retrievals, in order to assess the stand-alone predictability of the modelling system and its capability to be used in future emission scenarios.

Other data sets used as input for the calculations (country-level baseline mortality rates for the diseases and population data) have been taken from the WHO Global Health Observatory (www.who.int/gho/database/en/), being representative of the year 2010.

Concentration–response (C-R) functions: we use the methodology of Burnett *et al* (2014) that builds on the studies of Pope *et al* (2009, 2011) to constrain the shape of the C-R relationship by developing integrated exposure–response functions (IERs) using a wide range of mortality data capturing a vast range of air quality conditions. These IERs are employed to estimate relative risks attributable to ambient $PM_{2.5}$ for ischemic heart disease (IHD), cerebrovascular disease and related mortality from ischaemic and haemorrhagic stroke (CEVI and CEVH, respectively), chronic obstructive pulmonary disease (COPD), lung cancer (LC) and acute lower respiratory infection (ALRI). The RR is parameterised in the IER framework following the formulation:

$$RR(C) = 1 + a\left[1 - \exp(-\gamma\,(C - Co)^{\delta})\right] \text{ for } C > Co$$
$$RR = 1 \quad \text{for} \quad C \leq Co.$$

The theoretical minimum risk concentration, below which there is no evidence of health risks, is represented by the Co mass concentration. C is the measured concentration values of $PM_{2.5}$, and α, γ and δ are parameters that define the overall shape of the concentration–response relationship (Burnett *et al* 2014). The minimum risk exposure level for annual mean $PM_{2.5}$ adopted in the IER functions used in this study is 2.4–5.9 $\mu g\,m^{-3}$ (Cohen *et al* 2017).

Here we investigate the impact of several options related to $PM_{2.5}$ simulation and selection for the calculation of mortality estimates over Europe. As a first step, we focus on the role of horizontal grid spacing on the mortality rates of several diseases over Europe. We conducted two simulations of air quality over Europe; one with a 100 km horizontal resolution, adapting to the most recent resolution of global models (Lelieveld *et al* 2015), and another at a 20 km horizontal resolution that represents a widely-used regional scale configuration. Second, we analyse the uncertainties induced by the selection of surface versus 200 m layer averaged $PM_{2.5}$ concentrations to address the possible shortcomings of model simulations related to near-surface exchange processes.

A further key term in the calculation of the mortality rates is the RR factor, which is important for the estimation of burdens of disease under a wide range of aerosol concentrations. For this study we used the method of the global burden of disease for 2015 (Cohen *et al* 2017), which applied IER functions to account for health effects from very low to very high $PM_{2.5}$ concentrations (Burnett *et al* 2014). We calculate RR in 0.1 and 1 $\mu g\,m^{-3}$ mass concentration bins and discuss the range of uncertainties that these options might introduce into estimates of mortality rates. We calculated the RR from the exposure to air pollution for IHD, cerebrovascular disease (CEV), lower respiratory tract infections (LRIs) such as pneumonia, COPD and LC.

In addition, we calculated mortality and incidence rates of the aforementioned diseases using $PM_{2.5}$ concentrations derived by satellite retrievals, as described in van Donkelaar *et al* (2016), version V4.GL.02. In this dataset, $PM_{2.5}$ is estimated by combining AOD retrievals from the NASA MODIS, MISR, and SeaWIFS instruments with results from simulations of the GEOS-Chem chemical transport model, and subsequently calibrated to global ground-based observations of $PM_{2.5}$ using geographically weighted regression as detailed in van Donkelaar *et al* (2016). As mentioned by the developers, the datasets are gridded at the finest resolution of the information sources (0.1×0.1^{o}) that were incorporated, but do not fully resolve $PM_{2.5}$ gradients at the gridded resolution due to influence from information sources at coarser resolution. We used the dataset that refers to the year 2014 (the same as the model simulations) for $PM_{2.5}$ at 35% relative humidity, with dust and sea salt components removed from the total $PM_{2.5}$.

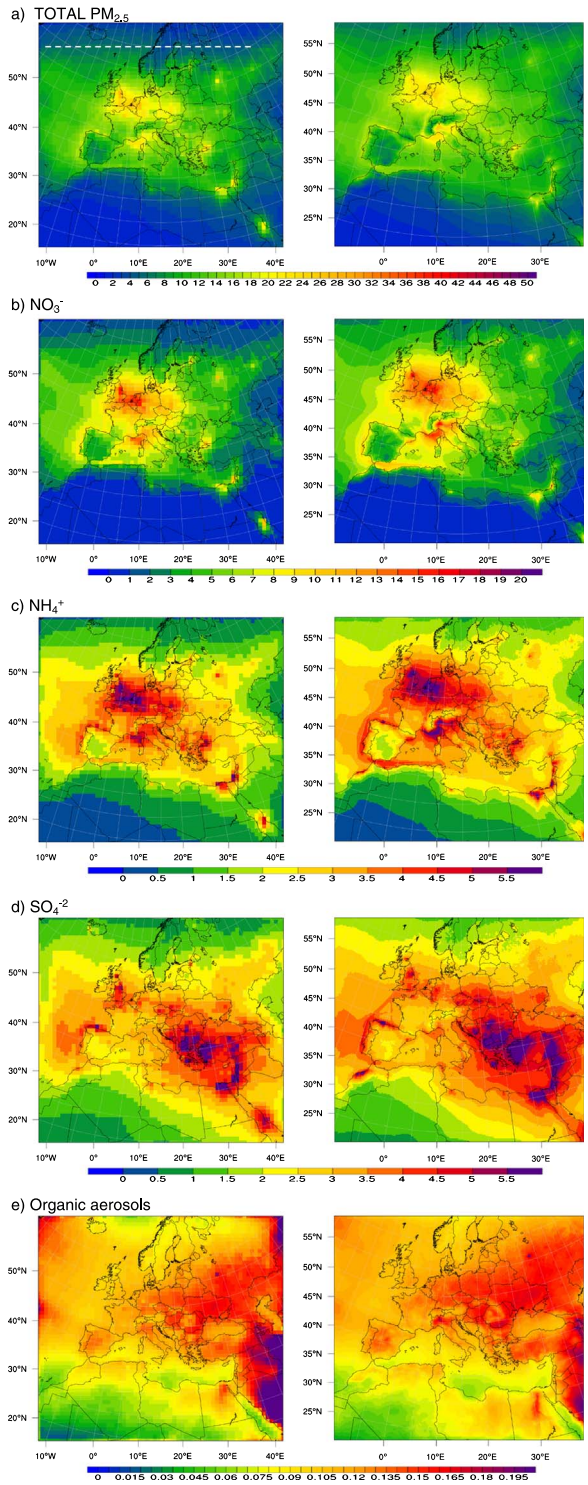

Figure 1. Annual mean concentrations ($\mu g\,m^{-3}$) for the year 2014 of (*a*) total $PM_{2.5}$, (*b*) NO_3^-, (*c*) NH_4^+, (*d*) SO_4^{-2} and (*e*) organic aerosols over the model domain. The white dashed line in the left panel of figure 1(*a*) defines the northern boundary of the Scandinavian countries (Finland, Sweden and Norway) up to which the country-based mortality estimates for domain 1 are calculated, in order not to include areas outside of domain 2. Left plots refer to the coarse domain (100 km grid spacing) while the right plots show the concentrations of $PM_{2.5}$ on the second domain with 20 km horizontal grid spacing.

3. $PM_{2.5}$ mean annual concentrations and comparison with observations

The mean annual $PM_{2.5}$ concentrations over Europe are depicted in figure 1(*a*). The left panels refer to results from the coarse resolution domain (100 km) while the right panels depict the $PM_{2.5}$ distribution as simulated in the fine resolution configuration (20 km). Central and north-west Europe are affected by the highest concentrations, along with specific hotspot areas such as the Po Valley in Italy and over several main eastern megacities, including Istanbul and Cairo.

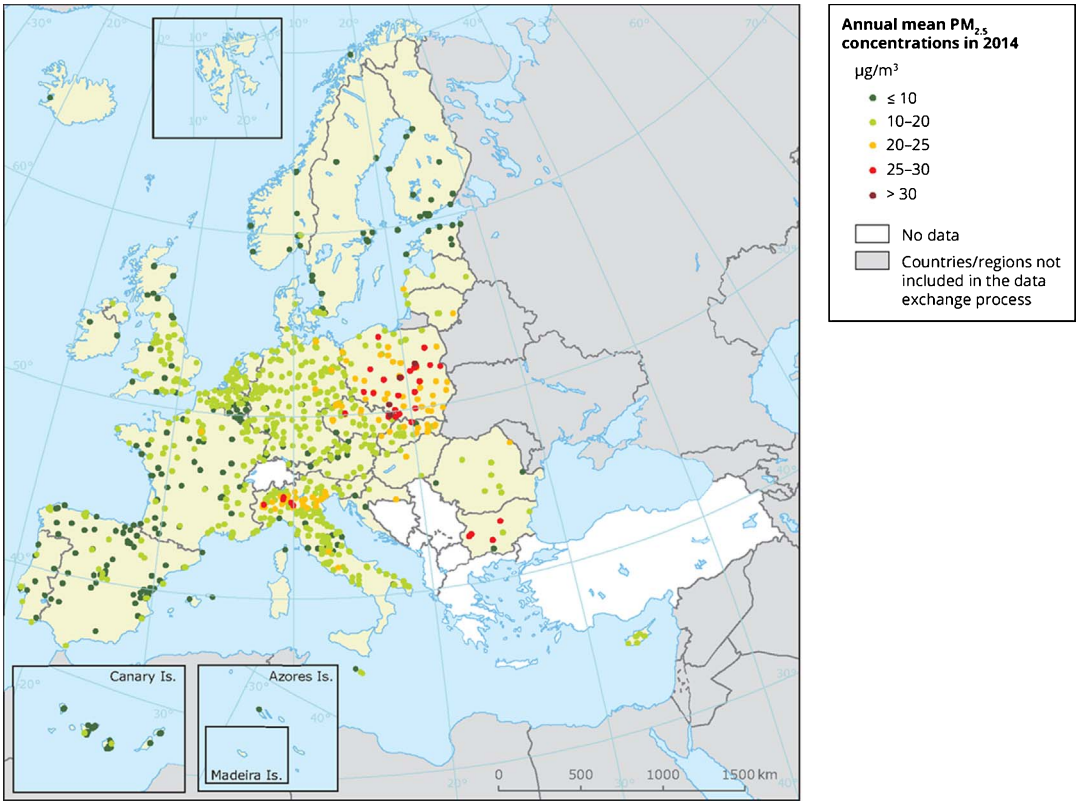

Figure 2. Annual mean $PM_{2.5}$ concentrations (in $\mu g\,m^{-3}$) for 2014 at background stations, based on daily averages with at least 75% of valid measurements (source: EEA, AirBase v.8 & AQ e-Reporting). The red and dark red dots indicate stations reporting concentrations above the EU annual target value ($25\,\mu g\,m^{-3}$). The dark green dots indicate stations reporting values below the WHO AQG for $PM_{2.5}$ ($10\,\mu g\,m^{-3}$). Only stations with $>$ 75% of valid data have been included (map www.eea.europa.eu/data-and-maps/figures/annual-mean-pm2-5-concentration-3).

Several inorganic sub-components of the total $PM_{2.5}$ are shown with the ammonium and nitrate components affecting mostly central and north-west Europe (figures 1(*b*) and (*c*)) while sulphates and organic aerosols are predominant over eastern and southern Europe (figures 1(*d*) and (*e*)). The mapped concentrations over the two domains reveal the details of the 20 km horizontal grid spacing, which is closer to the resolution of the emission inventory ($0.1 \times 0.1°$) to better capture a few hotspots of pollution such as in northern Italy, coastal cities and urban conglomerates. The analysis of the sub-components of the $PM_{2.5}$ distribution over Europe shows that in eastern and southern Europe, sulphate and organic carbon aerosols are the main contributors to the total anthropogenic fine particulate matter load. These regions are thus associated with a more acidic environment than central and western Europe; over the latter area, nitrate ammonium aerosols are more abundant. Despite that, in the current study, all the aerosol components are considered to have the same toxicological effect on human health, and the mortality estimates are calculated on the basis of total $PM_{2.5}$ mass. The speciation of $PM_{2.5}$ into distinct compounds might be of particular interest when information on the toxicity of individual aerosol components becomes available from epidemiological and toxicological studies. These graphs are also an indication that maximising the efficiency of emission reduction measures regarding health issues related to $PM_{2.5}$ might require accounting for their different spatiotemporal distribution.

A qualitative comparison of model results with observations (AirBase map of mean annual $PM_{2.5}$ concentrations in 2014, source: EEA 2016), as depicted in figure 2, shows several areas of over-estimation, mainly in the Benelux countries, northern Germany and northern France, and under-estimation over eastern European countries, mainly over Poland. The emission database used in this study, as mentioned, refers to emission rate estimates for 2010. It is plausible that concentrations of ground level pollution in central and northern Europe may have followed a reduction in particulate matter precursor and primary emissions, as reported in the report, Air Quality in Europe—2016 Report—European Environment Agency (www.eea.europa.eu/publications/air-quality-in-europe-2016/download). Figure 2.1(*a*) in that report depicts the development in EU-28 emissions during the period 2000–2014 (as a percentage of 2000 levels) of SO_X, NO_X, NH_3, PM_{10}, $PM_{2.5}$, NMVOCs, CO, CH_4 and BC), which is not reflected in the emission database used in this study.

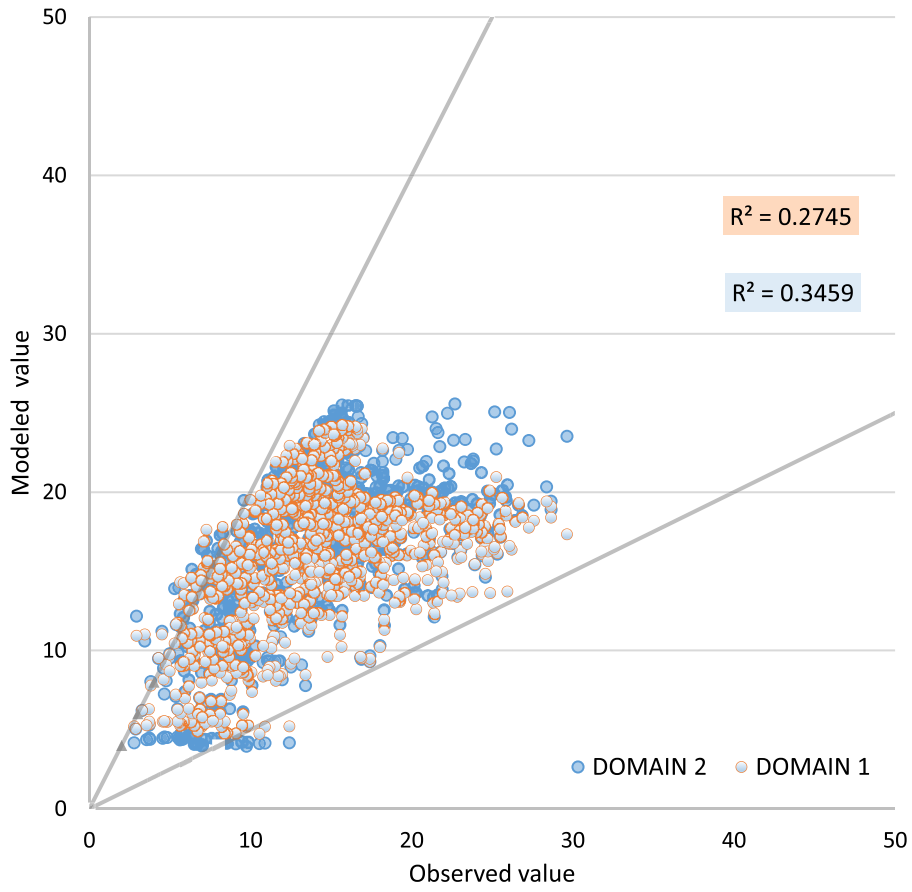

Figure 3. Modelled versus observed mean annual $PM_{2.5}$ concentrations over AirBase stations over Europe for 2014. The results from the coarse/fine domains (100km/20km horizontal grid spacing) are shown in orange/blue-contoured circles, respectively. The figure also includes the squared Pearson correlation coefficients R^2 of the linear least squares regression for both distributions (observations versus modelled values from first and second domains) with orange background for the coarse domain and blue background for the fine domain.

For a quantitative analysis, we compared the simulated and observed mean annual $PM_{2.5}$ concentrations for both domains (100 and 20 km) using measurements from the AIRBASE monitoring network, to test differences in agreement between measurements and simulations, and to investigate possible improvement from the 100 km domain ($R^2 = 0.27$) to the 20 km domain ($R^2 = 0.35$), as shown in figure 3. The results from the two domains differ slightly, with mean annual $PM_{2.5}$ concentrations of 16.3 $\mu g\,m^{-3}$ and 17.2 $\mu g\,m^{-3}$ over the coarse and fine grid domains, respectively. The averages of the station data from all AIRBASE stations included in the evaluation is 14.3 $\mu g\,m^{-3}$. Note that the stations do not necessarily represent mean concentrations across the entire model domain, especially because in the southern and eastern parts, ground station data are not available. The mean model bias at the station locations varies from 2 to 2.9 $\mu g\,m^{-3}$ from the 100 km to the 20 km resolution domain, and the root mean square error ranges from 6.4 to 6.6 $\mu g\,m^{-3}$ respectively. More than 95% of the data points fall within a factor of two (figure 3; grey lines) for both the coarse and fine resolution calculations.

4. Mortality estimates and uncertainties

We first calculated mortality rates for IHD, CEVI and CEVH, COPD, LC and ALRI over the region covered by the coarse grid resolution. The total mortality attributable to outdoor air pollution reaches 535 000 persons per year over the larger European domain (i.e. including some parts of North Africa and west Asia). Deaths per year due to LC and ALRI attributable to air pollution are about 37 000 and 34 000, respectively, followed by COPD, with 49 000 deaths (9% of the total deaths). The majority of deaths due to poor air quality are due to IHD (305 000) and CEV (108 000) that represent 57% and 20%, respectively, of the total deaths due to ambient aerosols (figure 4(*a*)). Recently, Lelieveld (2017) estimated the mortality attributable to air pollution in the EU-28 at about 274 000 deaths per year, while in this study we find 242 000–248 000 deaths per year, depending on model configuration. Differences between the two studies are attributed to the contributions made by ozone and natural dust particles, which are not included here. Both studies use a minimum risk exposure level distribution for annual mean $PM_{2.5}$, adopted in the IER functions of 2.4–5.9 $\mu g\,m^{-3}$.

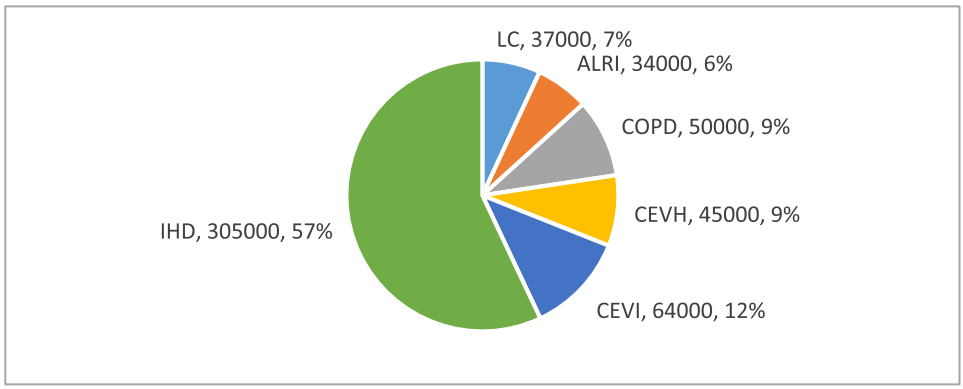

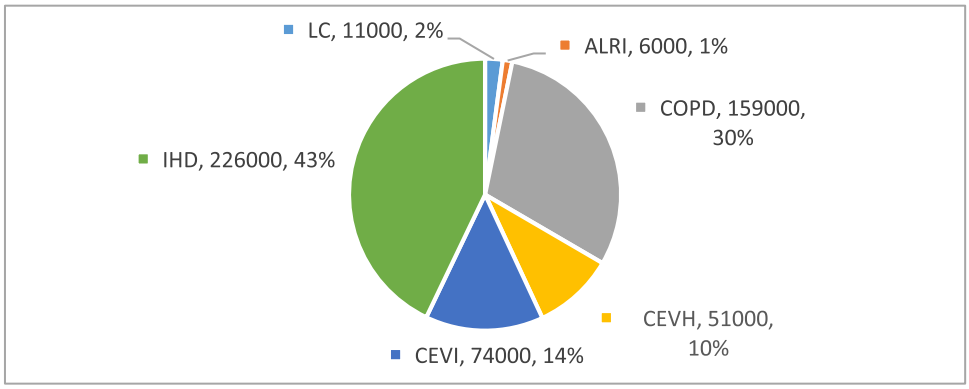

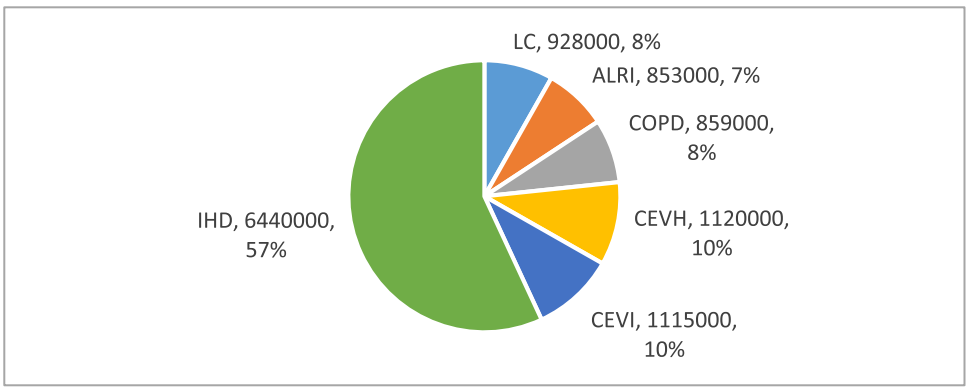

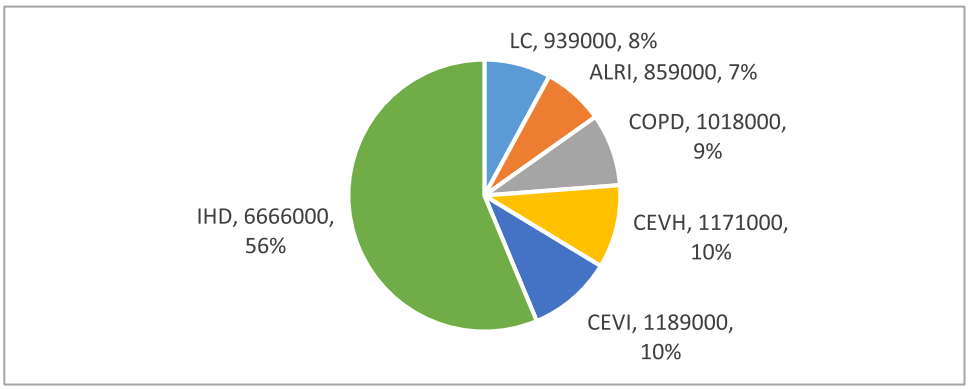

Figure 4. Estimates in total number and percentage of (*a*) mortality (number of deaths per year), (*b*) years of life with disability (YLD), (*c*) years of life lost (YLL) and (*d*) disability-adjusted life-years (DALYs) over the model domain for 2014 for the different disease categories.

In terms of years of life with disability (YLD), the majority is due to IHD with 226 000 years lost (43%) as shown in figure 4(*b*). CEV contributes a total of 125 000 YLD from both ischaemic and haemorrhagic stroke, representing 24% of total YLD over the domain. COPD has a larger relative contribution to YLD than to the mortality rates, reaching 30% of the years lost due to disease compared to a 9% contribution to the number of deaths. In contrast, LC and ALRI make a small contribution to the YLD over the region (2% and 1%, respectively) while the mortality rates due to these two diseases are a combined 14%. The number of years of life lost over the whole domain reaches 11.3 million in 2014, with half of that number being due to IHD.

The disability-adjusted life-years (DALYs), as a way of expressing the burden of disease in a population, is calculated as the sum of years of life lost (YLL) to premature mortality and the years of life with disability (YLD). Therefore, one DALY can be thought of as one healthy year of life lost. In our calculations, DALYs follow the disease-attributed distribution of the mortality estimates, with 56% of the total DALYs attributed to IHD, 20% to CEV, and 8%, 7% and 9% respectively to LC, ALRI and COPD. IHD claims more than 6.5 million years lost from mortality and living in disability due to the disease.

We also calculate the years of life lost from each cause of death as years of premature death (YPD):

$$\mathrm{YPD\,(i)} = \mathrm{YLL\,(i)}\,\frac{\mathrm{YLL\,(i)}}{\mathrm{M\,(i)}}$$

where YLL and M are the number of years lost and total mortality for each disease, and *i* is the respective disease. LC, ALRI and CEVH have the highest YPD, at 25 years, IHD is associated with 21 years, while COPD and CEVI have the lowest YPD, at 17 years.

Table 1 summarises all mortality rates derived from the different model configurations. The first column gives the population of the respective country. The second column shows the number of deaths per country as calculated from the ground level $PM_{2.5}$ concentrations of the coarse domain, with a grid spacing of 100 km. The third column presents the respective results with aerosol concentrations as simulated in the fine resolution domain (20 km). In the next column the concentrations of $PM_{2.5}$ are derived as an average value of the first three model layers below 200 m height above surface (L1 vs. L3). In all previous tests the RR parameter is calculated upon changes in $PM_{2.5}$ concentrations in 1 $\mu g\,m^{-3}$ steps. The fourth column shows the results where the RR parameter is calculated in concentration steps of 0.1 $\mu g\,m^{-3}$, i.e. ten values for each of the values assigned in the 1 $\mu g\,m^{-3}$ calculation, leading to a smoother RR distribution. Table 1 also includes the mortality rates per country based on $PM_{2.5}$ concentrations from satellite estimates, both with and without observational data assimilation. The last five columns show the difference in the mortality rates due to the use of coarse vs. fine chemical model resolution ((D1-D2) × 100/D1), $PM_{2.5}$ from surface vs. first three layers ((L1-L3) × 100/L1), 1 vs 0.1 $\mu g\,m^{-3}$ concentration steps in the calculation of RR ((RR1-RR01) × 100/RR1), as well as a comparison between model and satellite derived mortality rates ((Mod-Sat) × 100/Mod and (Mod-SatC) × 100/Mod). The countries are sorted in descending order of deaths per year. This listing highlights the countries with more pronounced collocations of high $PM_{2.5}$ concentrations and dense populations. This includes mainly eastern European countries such as Poland, Romania and Bulgaria.

When comparing the number of deaths based on the pollutant concentrations from the two domains, at country level, we obtain a minor but non-linear response for the mortality estimates, with most countries exhibiting lower mortality rates in the 100 km case than at $PM_{2.5}$ concentrations from the 20 km resolution domain (table 1). The reduced estimates at the coarse resolution domain over the entire domain reach –6% in Italy, –5% in Malta, −4.7% in Luxemburg, −7% in Slovenia and Spain and –9% in Portugal. In general, the countries with the largest biases cover small geographical areas, and the use of a higher resolution for $PM_{2.5}$ is important to represent national boundaries. Spain is the only larger country that exhibits a significant difference from the use of the 100 km versus the 20 km resolution domain. To a lesser extent, negative biases from the coarse grid are found for Bulgaria, France, Germany, Romania, and other countries. There are four countries (Denmark, Estonia, Latvia and the United Kingdom) where the use of the 100 km yields higher mortality rates than the 20 km domain. Overall, in the EU-28, the total mortality due to particulate matter pollution reaches 242 000–248 000 depending on model configuration. The uncertainty related to the use of the course versus fine resolutions is approximately ±2.4%. In this country-based comparison, for several countries (Finland, Sweden and Norway; highlighted with an asterisk in table 1) where the use of the larger domain (with 100 km grid spacing) includes larger areas of these countries, we limit the calculations to the northern boundary of the region defined by the second domain (the dashed line in figure 1(*a*)).

We perform the same country-based analysis by using $PM_{2.5}$ concentrations at ground level (L1) and concentrations averaged over the near-surface layer of approximately 200 m (L3) to test possible differences in the model results in view of the vertical exchange processes. The use of first layer or 200 m layer $PM_{2.5}$ concentrations yields statistically insignificant differences in mortality estimates, with most of the countries exhibiting uncertainties of less than 1% (0.58%). The use of the ground level concentrations leads, in general, to slightly higher mortality rates related to the slightly higher $PM_{2.5}$ levels at the surface compared to the 200 m average concentration.

Table 1. Country name, population (column 2), mortality (deaths per year) estimates per country derived from model (four configurations: columns 3–6) and satellite (two configurations: columns 7–8) $PM_{2.5}$ concentrations and relative uncertainties (columns 9–13).

COUNTRY	Population ($\times 10^3$)	100 km Domain D1	20 km Domain D2	200 m (L3) lowest layer	D1 with RR 0.1μg bins	Satellite data	Satellite data ass.	(D1-D2) ×100/D1	(L1 L 3) ×100/L1	(RR1-RR0.1) ×100/RR1	(Mod-Sat) ×100/Mod	(Mod-Sat_data ass.) ×100/Mod
Germany	80435	52823	53708	53532	53167	47993	45991	−1.67	0.33	1	9.73	13.49
Italy	59588	28423	30128	29824	29733	25650	27529	−6	1.01	1.31	13.73	7.41
Poland	38575	26207	26326	26225	26019	27380	27374	−0.45	0.38	1.18	−5.23	−5.21
France	62961	21138	21670	21385	21393	14709	15536	−2.52	1.31	1.27	31.24	27.38
Romania	20299	17669	18236	18203	17994	19915	17815	−3.21	0.18	1.35	−10.67	0.99
Spain	46601	12871	13784	13614	13480	8783	9452	−7.09	1.23	2.25	34.84	29.88
Hungary	10014	8844	8923	8918	8798	9077	8656	−0.89	0.05	1.4	−3.17	1.61
Netherlands	16632	8552	8676	8546	8596	6748	6329	−1.45	1.49	0.93	21.49	26.37
Bulgaria	7407	8081	8259	8230	8149	7996	7237	−2.21	0.34	1.32	1.87	11.19
Czechia	10507	7837	7954	7917	7870	7711	7648	−1.49	0.46	1.04	2.02	2.82
Belgium	10930	6878	6978	6872	6908	5237	4994	−1.45	1.52	1	24.2	27.71
Greece	11178	6615	6639	6571	6527	4402	4344	−0.35	1.01	1.67	32.55	33.44
Portugal	10585	4660	5086	4973	5006	2876	2900	−9.14	2.21	1.6	42.55	42.07
Austria	8392	4092	4127	4152	4071	3849	4068	−0.84	−0.61	1.35	5.5	0.07
Slovakia	5407	4088	4105	4107	4061	4073	4040	−0.41	−0.07	1.07	−0.29	0.52
Sweden*	9382	3605	3576	3645	3459	4064	3869	0.81	−1.95	3.38	−17.49	−11.85
Croatia	4316	3115	3187	3195	3147	2796	2803	−2.33	−0.25	1.27	11.15	10.93
Switzerland	7831	2733	2718	2716	2673	2660	3020	0.57	0.04	1.67	0.48	−12.98
Denmark	5550	2732	2682	2669	2641	2070	1949	1.83	0.51	1.51	21.62	26.2
Lithuania	3123	2699	2708	2736	2658	3204	3056	−0.33	−1	1.85	−20.54	−14.97
Latvia	2090	1825	1821	1832	1787	2096	1991	0.22	−0.6	1.88	−17.29	−11.41
Finland*	5367	1675	1694	1693	1634	1935	1818	−1.1	0.08	3.54	−18.42	−11.26
Ireland	4617	1359	1360	1360	1335	478	478	−0.05	0	1.81	64.19	64.19
Norway*	4890	1332	1360	1362	1303	978	928	−2.01	−0.19	4.34	24.94	28.78
Slovenia	2051	1026	1100	1097	1085	925	990	−7.24	0.25	1.38	14.74	8.75
Estonia	1332	849	830	829	814	909	838	2.2	0.02	1.92	−11.67	−2.95
Cyprus	1104	266	273	273	265	241	228	−2.76	0.13	2.94	9.51	13.96
Luxembourg	508	197	207	202	205	150	142	−4.73	1.97	0.57	26.83	30.73
Malta	412	135	142	138	139	21	10	−5.07	2.9	2.29	84.89	92.8
TOTAL	**452084**	**242326**	**248257**	**246816**	**244917**	**218926**	**217034**	**−2.4%**	**0.58%**	**0.77%**	**10.6%**	**11.4%**

Table 2. Premature deaths per year for each disease category (LC, ALRI, COPD, CEVH, CEVI and IHD), and totals based on modelled $PM_{2.5}$ concentrations (four configurations) over Europe. MIN and MAX columns represent the range of values of the 95% confidence intervals from epidemiological data.

Deaths Disease	MIN	D1 100 km L3 average	D2 20 km L3 average	D2 20 km L1 average	D2 20 km L3 average 0.1 μg bins	MAX
LC	27 825	37 375	38 683	39 250	37 875	48 905
ALRI	22 517	34 265	35 787	36 466	35 009	47 678
COPD	34 275	49 537	50 979	51 561	50 108	65 757
CEVH	26 472	44 780	45 923	46 332	45 215	63 657
CEVI	37 337	64 251	65 477	65 947	64 387	91 327
IHD	211 477	305 316	310 343	312 175	306 325	400 622
ALL	359 903	535 524	547 192	551 731	538 919	717 946

We also compare the mortality estimates as derived using RR calculations based on 1 and 0.1 $\mu g\,m^{-3}$ concentrations bins. The calculation of RR in 1 $\mu g\,m^{-3}$ bins yields higher mortality rates than the $RR_{0.1}$, with differences reaching 2.9% over Cyprus and 3.5% over Finland, 3.3% over Sweden and 4.3% over Norway. However, in total over the EU-28, the differences in the annual number of deaths from particulate matter pollution, driven by the resolution of the RR calculation, are within 0.8%.

We additionally calculated mortality rates based on $PM_{2.5}$ concentrations derived from satellite observations, with and without assimilation of ground observational data, as described in van Donkelaar *et al* (2016). In general, satellite-derived aerosol levels yield approximately 10% lower mortality rates over the EU-28. The use of the assimilated $PM_{2.5}$ values leads to improved agreement between the satellite-based mortality results and the results of our regional model, which in the present application does not use data assimilation. Apart from Germany, in the top ten countries and in terms of deaths per year rates, the data assimilation process in the satellite output brings satellite mortality rates closer to our model results by either reducing or increasing the non-corrected satellite driven estimates. This is particularly evident in six of the top seven countries, which account for almost half of the premature deaths in EU-28 (Italy, Poland, France, Romania, Spain, and Hungary).

For a domain-wide analysis, we mask the mortality estimates delivered from the coarse domain to produce only mortality rates for the grid cells included in the fine domain in order to compare similar areas. From this comparison, as summarised in table 2, over the entire domain (the European continent, including parts of west Asia and North Africa) the deaths due to air pollution reach over half a million people per year. The different configuration modes slightly alter the mortality estimates over the domain, with values varying from 535 000 to 552 000 deaths per year, while the uncertainties from epidemiological data lead to a range of 360 000–718 000 annual deaths (95% confidence interval).

In figure 6 we summarise all uncertainties in mortality rates that can be attributed to model configuration (domain grid spacing–grey columns; vertical level–yellow columns; and RR concentration bins–green columns) and the uncertainties introduced by the range of the epidemiological data that define the relative risk of disease, shown by the minimum (light blue) and maximum (light red) values of RR (95% confidence interval). The uncertainties (U) are calculated, per disease and in total, as follows.

95% uncertainty interval lower IER:

$$\mathrm{U\,(IERmin)} = \frac{\mathrm{M\,(RRave)} - \mathrm{M\,(RRmin)}}{\mathrm{M\,(RRave)}} \times 100\%$$

95% uncertainty interval higher IER:

$$\mathrm{U\,(IERmax)} = \frac{\mathrm{M\,(RRave)} - \mathrm{M\,(RRmax)}}{\mathrm{M\,(RRave)}} \times 100\%$$

Horizontal resolution (HR) uncertainty:

$$\mathrm{U\,(HR)} = \frac{\mathrm{M\,(D01)} - \mathrm{M\,(D02)}}{\mathrm{M\,(D01)}} \times 100\%$$

Vertical resolution (VR) uncertainty:

$$\mathrm{U\,(VR)} = \frac{\mathrm{M\,(L3)} - \mathrm{M\,(L1)}}{\mathrm{M\,(L3)}} \times 100\%$$

RR concentration step (RR) uncertainty:

$$\mathrm{U\,(RR)} = \frac{\mathrm{M\,(1)} - \mathrm{M\,(01)}}{\mathrm{M\,(1)}} \times 100\%$$

where M is the mortality estimate for each case, D01 and D02 are respectively the coarse and fine grid domains, L3 and L1 are the averaged three first levels and ground level model results, and 1 and 01 are the mortality estimates from the calculation of the relative risk in the 1 $\mu g\,m^{-3}$ and 0.1 $\mu g\,m^{-3}$ concentration bins.

Figure 6 illustrates that the uncertainties due to domain configurations vary from −3.5% to 2.1% for LC, −4.4% to 2.2% for ALRI, −2.9% to 1.7% for COPD, −2.6% to 1.5% for CEVH, −1.9% to 1.7% for CEVI and −1.6% to 1.3% for IHD, averaging over all diseases to −2.2% to 1.5%, with the negative values attributed to the impact of higher resolution and the positive values attributed to the impact of the smaller concentrations size bin for the calculation of RR (0.1 $\mu g\,m^{-3}$ versus 1 $\mu g\,m^{-3}$). The uncertainties from the use of the 95% confidence interval (minimum and maximum values) of RR reach +25% to −31% for LC, +34% to −39% for ALRI, 31% to −33% for COPD, 41% to −42% for CEVH and CEVI, ±31% for IHD,

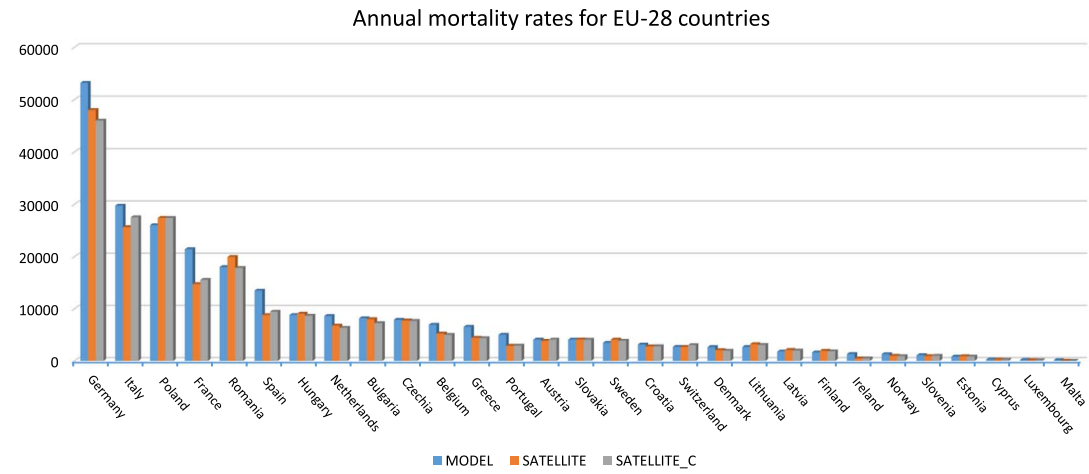

Figure 5. Annual premature mortality rates for EU-28 countries derived from $PM_{2.5}$ concentrations from the model (blue columns), satellite estimates without correction through data assimilation (orange columns) and satellite estimates with observational data assimilation (grey columns).

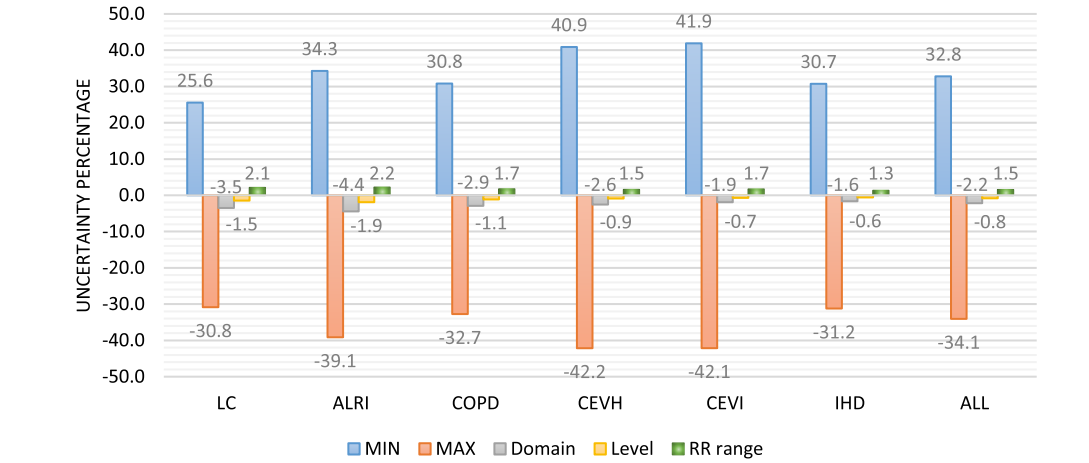

Figure 6. Uncertainties in mortality estimates related to model configuration (domain grid spacing in grey, level of $PM_{2.5}$ concentration in yellow), RR concentrations step (in green) and the 95% confidence interval in IER functions (lower range in blue and upper range in red) for each disease and in total.

and an average IER uncertainty between +32.8% and −34.1%. We conclude that the domain-wide average differences in mortality rates that can be attributed to model configuration are significantly smaller than the uncertainties of the epidemiological data that define the relative risk of disease within the 95% confidence interval.

5. Conclusions

We performed several sensitivity tests to calculate mortality rates over Europe. We used a regional coupled air quality model (WRF-Chem) with two domains at 100 km and 20 km grid resolutions, respectively, to simulate $PM_{2.5}$ concentrations and, in turn, the number of premature deaths per year attributed to aerosols for IHD, CEV, LRIs such as pneumonia, COPD and LC. The base mortality rates are calculated based on ground $PM_{2.5}$ concentrations for both domains. We also used 200 m above ground average $PM_{2.5}$ to account for possible shortcomings of model simulations related to near-surface exchange processes. Additionally, we calculated the relative risk factor in 1 $\mu g\,m^{-3}$ and 0.1 $\mu g\,m^{-3}$ concentration bins for a smoother distribution of relative risk (RR).

The mortality rates differ by 2.4% due to horizontal resolution of the model configuration, by 0.6% due to the vertical distribution of $PM_{2.5}$, and by 0.8% due to the resolution of RR. Estimates based on $PM_{2.5}$ concentrations derived from satellite data are within 10% of the model results. The use of data assimilation in the satellite estimates brings mortality rates for most of the countries having high death rates closer to the model results. On the other hand, the 95% confidence intervals of the IER functions for these diseases give rise to statistical uncertainties in the estimates within about ± 30%. These results indicate that the uncertainties of mortality estimates are dominated by the estimated response of population

to air pollution, derived from epidemiological data, rather than the representation of annual mean $PM_{2.5}$ values by air quality models and/or observations.

Acknowledgments

The computational resources and support were provided by the European Union Horizon 2020 research and innovation programme VI-SEEM project under grant agreement 675121. The near-surface $PM_{2.5}$ distributions based on satellite data can be accessed at the Atmospheric Composition Analysis Group of the Department of Physics and Atmospheric Science, Dalhousie University, (http://fizz.phys.dal.ca/~atmos/martin/?page_id=140). The aerosol measurements are derived from the AirBase European-wide air quality database hosted by the European Environmental Agency (EEA) that contains validated air quality monitoring information for more than 30 participating countries throughout Europe (available at http://aidef.apps.eea.europa.eu, www.eea.europa.eu/data-and-maps/). We acknowledge the use of the anthropogenic emission datasets downloaded from http://edgar.jrc.ec.europa.eu/htap_v2/. The emissions were prepared in the framework of the Task Force on Hemispheric Transport of Air Pollution (TF-HTAP) organised in 2005 under the auspices of the UNECE Convention on Long-range Transboundary Air Pollution (LRTAP Convention). The authors would also like to thank the two anonymous referees for their reviews and constructive comments.

ORCID iDs

Jonilda Kushta https://orcid.org/0000-0003-3695-9267
Andrea Pozzer https://orcid.org/0000-0003-2440-6104
Jos Lelieveld https://orcid.org/0000-0001-6307-3846

References

Ackermann I J, Hass H, Memmesheimer M, Ebel A, Binkowski F S and Shankar U 1998 Modal aerosol dynamics model for Europe: development and first applications *Atmos. Environ.* **32** 2981–99

Anenberg S C, Horowitz L W, Tong D Q and West J J 2010 An estimate of the global burden of anthropogenic ozone and fine particulate matter on premature human mortality using atmospheric modeling *Environ. Health Perspect.* **118** 1189–95

Anenberg S C *et al* 2012 Global air quality and health co-benefits of mitigating near-term climate change through methane and black carbon emission controls *Environ. Health Perspect.* **120** 831–9

Beelen R *et al* 2014 Effects of long-term exposure to air pollution on natural-cause mortality: an analysis of 22 European cohorts within the multicentre ESCAPE project *Lancet* **383** 785–95

Bey I, Jacob D J, Yantosca R M, Logan J A, Field B D, Fiore A M, Li Q, Liu H, Mickley L J and Schultz M G 2001 Global modeling of tropospheric chemistry with assimilated meteorology: model description and evaluation *J. Geophys. Res. Atmos.* **106** 23073–95

Burnett R T *et al* 2014 An integrated risk function for estimating the global burden of disease attributable to ambient fine particulate matter exposure *Environ. Health Perspect.* **122** 397–403

Chen F and Dudhia J 2001 Coupling an advanced land surface hydrology model with the penn state-NCAR MM5 modeling system. Part I: model implementation and sensitivity *Mon. Weather Rev.* **129** 569–85

Cohen A J *et al* 2005 The global burden of disease due to outdoor air pollution *J. Toxic. Environ. Health A.* **68** 1301–7

Cohen A J *et al* 2017 Estimates and 25-year trends of the global burden of disease attributable to ambient air pollution: an analysis of data from the global burden of diseases study 2015 *Lancet* **389** 1907–18

Dockery D W, Pope C A III, Xu X, Spengler J D, Ware J H, Fay M E, Ferris B G Jr and Speizer F E 1993 An association between air pollution and mortality in six US cities *N. Engl. J. Med.* **329** 1753–9

Dockery D W 2009 Health effects of particulate air pollution *Ann. Epidemiol.* **19** 257–63

EEA 2016 Air quality in Europe—2016 report (www.eea.europa.eu/publications/air-qualityin-europe-2016/download)

Emmons L K *et al* 2010 Description and evaluation of the model for ozone and related chemical tracers, version 4 (MOZART-4) *Geosci. Model Dev.* **3** 43–67

Fast J D, Gustafson W I Jr, Easter R C, Zaveri R A, Barnard J C, Chapman E G and Grell G A 2006 Evolution of ozone, particulates, and aerosol direct forcing in an urban area using a new fully-coupled meteorology, chemistry, and aerosol model *J. Geophys. Res. Atmos.* **111** D21305

Fann N, Lamson A D, Anenberg S C, Wesson K, Risley D and Hubbell B J 2012 Estimating the national public health burden associated with exposure to ambient $PM_{2.5}$ and ozone *Risk Anal.* **32** 81–95

Filleul L *et al* 2005 Twenty-five year mortality and air pollution: results from the French PAARC survey *Occup. Environ. Med.* **62** 453–60

Giannadaki D, Lelieveld J and Pozzer A 2017 *The Impact of Fine Particulate Outdoor Air Pollution to Premature Mortality* (New York: Springer)

Grell G A and Devenyi D 2002 A generalized approach to parameterizing convection combining ensemble and data assimilation techniques *Geophys. Res. Lett.* **29** 10–3

Grell G A, Peckham S E, Schmitz R, McKeen S A, Frost G, Skamarock W C and Eder B 2005 Fully coupled 'online' chemistry within the WRF model *Atmos. Environ.* **39** 6957–75

Hong S-Y, Noh Y and Dudhia J 2006 A new vertical diffusion package with an explicit treatment of entrainment processes *Mon. Wea. Rev.* **134** 2318–41

Iacono M J, Delamere J S, Mlawer E J, Shephard M W, Clough S A and Collins W D 2008 Radiative forcing by long-lived greenhouse gases: calculations with the AER radiative transfer models *J. Geophys. Res. Atmos.* **113** D13103

Janssens-Maenhout G *et al* 2012 *EDGAR-HTAP: A Harmonized Gridded Air Pollution Emission Dataset Based on National Inventories* (Luxemburg: European Commission, Joint Research Centre, Institute for Environment and Sustainability)

Krewski D *et al* 2009 *Extended Follow-Up and Spatial Analysis of the American Cancer Society Study Linking Particulate Air Pollution and Mortality* (Boston, MA: HEI Research Report 140. Health Effects Institute)

Lelieveld J, Evans J S, Fnais M, Giannadaki D and Pozzer A 2015 The contribution of outdoor air pollution sources to premature mortality on a global scale *Nature* **525** 367–71

Lelieveld J 2017 Clean air in the anthropocene *Faraday Discuss.* **2017** 693–703

Li Y *et al* 2010 Burden of disease attributed to anthropogenic air pollution in the United Arab Emirates: estimates based on observed air quality data *Sci. Total Environ.* **408** 5784–93

Middleton P, Stockwell W R and Carter W P L 1990 Aggregation and analysis of volatile organic compound emissions for regional modelling *Atmos. Environ.* **24** 1107–23

Morrison H, Curry J A and Khvorostyanov V I 2005 A new double-moment microphysics parameterization for application in cloud and climate models. Part I: Description *J. Atmos. Sci.* **62** 1665–77

Ostro B *et al* 2010 Long-term exposure to constituents of fine particulate air pollution and mortality: results from the California teachers study *Environ. Health Perspect.* **118** 363–9

Pope C A III *et al* 2002 Lung cancer, cardiopulmonary mortality, and long-term exposure to fine particulate air pollution *J. Am. Med. Assoc.* **287** 1132–41

Pope C A III *et al* 2004 Cardiovascular mortality and long-term exposure to particulate air pollution: epidemiological evidence of general pathophysiological pathways of disease *Circulation* **109** 71–7

Pope C A III, Ezzati M and Dockery D W 2009 Fine-particulate air pollution and life expectancy in the United States *N. Engl. J. Med.* **360** 376–86

Pope C A, Burnett R T, Turner M C, Cohen A, Krewski D, Jerrett M, Gapstur S M and Thun M J 2011 Lung cancer and cardiovascular disease mortality associated with ambient air pollution and cigarette smoke: Shape of the exposure-response relationships *Environ. Health Perspect.* **119** 1616–21

Pozzer A, Zimmermann P, Doering U M, van Aardenne J, Tost H, Dentener F, Janssens-Maenhout G and Lelieveld J 2012 Effects of business-as-usual anthropogenic emissions on air quality *Atmos. Chem. Phys.* **12** 6915–37

Pozzer A, Tsimpidi A P, Karydis V A, de Meij A and Lelieveld J 2017 Impact of agricultural emission reductions on fine-particulate matter and public health *Atmos. Chem. Phys.* **17** 12813–26

Punger E M and West J J 2013 The effect of grid resolution on estimates of the burden of ozone and fine particulate matter on premature mortality in the USA *Air Qual. Atmos. Health* **6** 563–73

Rückerl R, Schneider A, Breitner S, Cyrys J and Peters A 2011 Health effects of particulate air pollution: a review of epidemiological evidence *Inhalat Toxicol* **23** 555–92

Schell B, Ackermann I J, Hass H, Binkowski F S and Ebel A 2001 Modeling the formation of secondary organic aerosol within a comprehensive air quality model system *J. Geophys. Res.* **106** 28275–93

Stockwell W R, Middleton P, Chang J S and Tang X 1990 The second generation regional acid deposition model chemical mechanism for regional air quality modelling *J. Geophys. Res.* **95** 16343–67

Thompson T M, Saari R K and Selin N E 2014 Air quality resolution for health impact assessment: influence of regional characteristics *Atmos. Chem. Phys.* **14** 969–78

US Environmental Protection Agency 2007 EPA-454/B-07-002. Research Triangle Park, NC: 2007. Guidance on the use of models and other analyses for demonstrating attainment of air quality goals for ozone, $PM_{2.5}$, and regional haze

van Donkelaar A, Martin R V, Brauer M, Hsu N C, Kahn R A, Levy R C, Lyapustin A, Sayer A M and Winker D M 2016 Global estimates of fine particulate matter using a combined geophysical-statistical method with information from satellites, models, and monitors *Environ. Sci. Technol.* **50** 3762–72

West J J, Fiore A M, Horowitz L W and Mauzerall D L 2006 Global health benefits of mitigating ozone pollution with methane emission controls *Proc. Natl Acad. Sci. USA* **103** 3988–93

Zhang D and Anthes R A 1982 High-resolution model of the planetary boundary layer—sensitivity tests and comparisons with SESAME-79 data *J. Appl. Meteorol.* **21** 1594–609